



**HAL**  
open science

## Review of statistical energy analysis hypotheses in vibroacoustics

Thibault Lafont, Nicolas Totaro, Alain Le Bot

► **To cite this version:**

Thibault Lafont, Nicolas Totaro, Alain Le Bot. Review of statistical energy analysis hypotheses in vibroacoustics. Proceedings of the Royal Society A: Mathematical, Physical and Engineering Sciences, 2014, 470, pp.20130515. 10.1098/rspa.2013.0515 . hal-00918078

**HAL Id: hal-00918078**

**<https://hal.science/hal-00918078>**

Submitted on 13 Dec 2013

**HAL** is a multi-disciplinary open access archive for the deposit and dissemination of scientific research documents, whether they are published or not. The documents may come from teaching and research institutions in France or abroad, or from public or private research centers.

L'archive ouverte pluridisciplinaire **HAL**, est destinée au dépôt et à la diffusion de documents scientifiques de niveau recherche, publiés ou non, émanant des établissements d'enseignement et de recherche français ou étrangers, des laboratoires publics ou privés.

## Research

Article submitted to journal

### Subject Areas:

Acoustics, Statistical physics

### Keywords:

statistical energy analysis, diffuse field, energy equipartition, rain-on-the-roof excitation

### Author for correspondence:

Thibault Lafont

e-mail: [thibault.lafont@cpe.fr](mailto:thibault.lafont@cpe.fr)

# Review of statistical energy analysis hypotheses in vibro-acoustics

T. Lafont<sup>1,2</sup>, N. Totaro<sup>2</sup> and A. Le Bot<sup>1</sup>

<sup>1</sup>Laboratoire de Tribologie et Dynamique des Systemes, Ecole Centrale de Lyon, 36 Avenue Guy de Collongues, F69134 Ecully Cedex, France

<sup>2</sup>Laboratoire Vibrations Acoustique, INSA-Lyon, Batiment St Exupery, 25 bis Avenue Jean Capelle, F69621 Villeurbanne Cedex, France

This paper is a discussion on the equivalence between rain-on-the-roof excitation, diffuse field and modal energy equipartition hypotheses when using statistical energy analysis (SEA). A first example of a simply supported plate is taken to quantify whether a field is diffuse or the energy is equally distributed among modes. It is shown that the field can be diffuse in a certain region of the frequency-damping domain with a single point force but without energy equipartition. For a rain-on-the-roof excitation the energy becomes equally distributed and the diffuse field is enforced in all regions. A second example of two plates coupled by a light spring is discussed. It is shown that in addition to previous conclusions, the power exchanged between plates agrees with the statistical prediction of SEA if and only if the field is diffuse. The special case of energy equipartition confirms this observation.

## 1. Introduction

The statistical energy analysis (SEA) is a method introduced by Lyon [1] in the sixties intended to estimate the vibroacoustic response of complex structures in the high frequency range by a statistical approach. This is the analogous of statistical mechanics for structural dynamics and as such could be called statistical vibroacoustics [2,3]. However, the difficulties encountered when using SEA for engineering purpose have motivated many studies on the required assumptions and have scattered the opinions of the scientific community on their status.

The main result of SEA is the so-called "coupling power proportionality". It states that the mean power exchanged between two subsystems is proportional to the difference of modal energies. The modal energy thus plays the role of vibrational temperature and the "convective coefficient" is called coupling loss factor. Regarding the foundations, there are several manners to approach SEA: the modal and the wave approaches. Fahy [4] gives a retrospective for each one. The modal approach of SEA starts from basic equations of mechanical oscillators excited by random forces and proves the existence of the coupling loss factors [5–7]; whereas the wave approach is based on the evaluation of the reflection and transmission coefficients at a junction [8–10] (considering plane waves) and provides effective relationships for the coupling loss factors. Using these concepts, the question of the equivalence between the hypotheses used in both approaches is raised.

The present work is a discussion on the assumptions of energy equipartition, rain-on-the-roof and diffuse field. For that purpose, the two approaches are reviewed to highlight the usefulness of the assumptions in the derivation of the coupling power proportionality equation. The example of a simply supported plate is taken to evaluate the conditions to fulfill these assumptions; the second example carried out on a two coupled plates system is set up to compare SEA coupling power proportionality with the previous conditions.

## 2. Basics of SEA

The simplest system for which the coupling power proportionality may be stated consists in two mechanical oscillators submitted to uncorrelated random forces as shown in Figure 1. The state is described by a unique variable  $X_i$  for the position of oscillator  $i$ . The governing equations are,

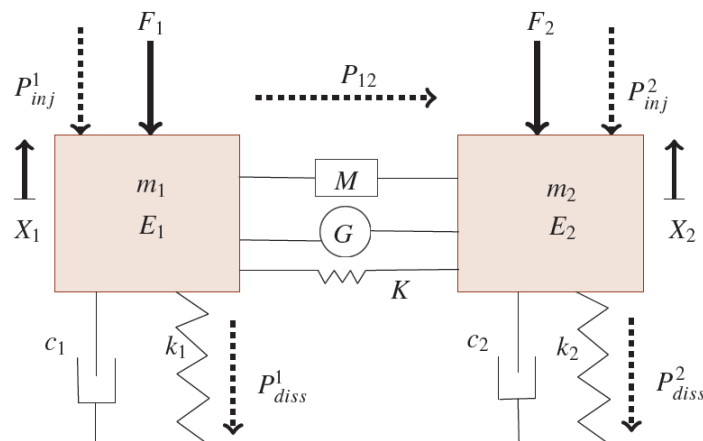


**Figure 1.** Two oscillators having mass  $m_i$ , stiffness  $k_i$  and damping  $c_i$  are coupled by an inertial  $M$ , an elastic  $K$  and a gyroscopic  $G$  couplings excited by uncorrelated random forces  $F_i$ .

$$\begin{aligned} m_1 \ddot{X}_1 + M \ddot{X}_2 + c_1 \dot{X}_1 + G \dot{X}_2 + k_1 X_1 + K(X_1 - X_2) &= F_1, \\ m_2 \ddot{X}_2 + M \ddot{X}_1 + c_2 \dot{X}_2 - G \dot{X}_1 + k_2 X_2 + K(X_2 - X_1) &= F_2, \end{aligned} \quad (2.1)$$

where  $m_i$  are the masses,  $c_i$  the viscous damping coefficients and  $k_i$  the spring stiffnesses of oscillators. The oscillators are coupled through three constants  $M$ ,  $G$  and  $K$  for respectively inertial, gyroscopic and elastic couplings. These three kinds of coupling forces ensure that no dissipation occurs in the coupling. With this respect, the first assumption of statistical energy analysis is that *the coupling is conservative*. The external forces  $F_i$  are assumed to be random. More exactly, the second assumption of statistical energy analysis is that *the forces are uncorrelated white*

noises. In particular the power spectral densities are constant over the whole frequency band and the cross power density is null. Under these conditions, it is proved by Lyon and Maidanik [5] and Lyon and Scharon [11] that the expectation of the power flow between oscillators is proportional to the difference in the expectation of vibrational energies,

$$\langle P_{12} \rangle = \beta (\langle E_1 \rangle - \langle E_2 \rangle), \quad (2.2)$$

where the brackets  $\langle . \rangle$  indicate a probability expectation. This is the coupling power proportionality. The coefficient  $\beta$  is,

$$\beta = \frac{\mu^2 (\Delta_1 \Omega_2^4 + \Delta_2 \Omega_1^4 + \Delta_1 \Delta_2 (\Delta_1 \Omega_2^2 + \Delta_2 \Omega_1^2)) + (\gamma^2 + 2\mu\kappa) (\Delta_1 \Omega_2^2 + \Delta_2 \Omega_1^2) + \kappa^2 (\Delta_1 + \Delta_2)}{(1 - \mu^2) [(\Omega_1^2 - \Omega_2^2)^2 + (\Delta_1 + \Delta_2) (\Delta_1 \Omega_2^2 + \Delta_2 \Omega_1^2)]}, \quad (2.3)$$

where  $\Omega_i^2 = (k_i + K)/m_i$ ,  $\Delta_i = c_i/m_i$ ,  $\mu = M/\sqrt{m_1 m_2}$ ,  $\gamma = G/\sqrt{m_1 m_2}$  and  $\kappa = K/\sqrt{m_1 m_2}$ .

A generalization to an arbitrary number of oscillators is achieved by Newland [12] who introduced the perturbation technique. Defining a small parameter  $\epsilon$  for the strength of coupling, the asymptotic developments of  $\langle P_{12} \rangle$  and  $\langle E_i \rangle$  in powers of  $\epsilon$  leads to a direct comparison of  $\langle P_{12} \rangle$  and  $\langle E_1 \rangle - \langle E_2 \rangle$ . The coupling power proportionality as given in equation (2.2) remains valid up to order two in  $\epsilon$  for any pair of oscillators with  $\beta$  as in equation (2.3) provided that *the coupling is assumed to be weak*. This is the third assumption in statistical energy analysis.

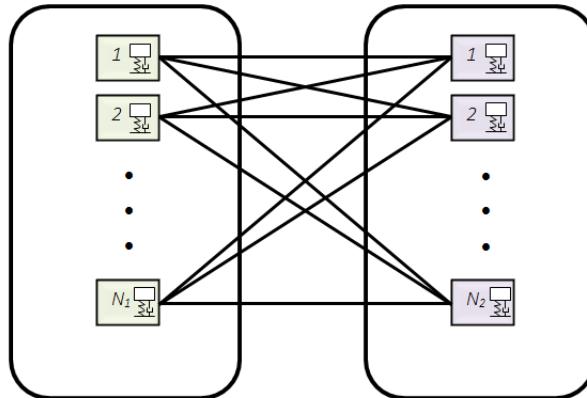


**Figure 2.** Energy exchanges between two subsystems containing oscillators.

The coupling power proportionality also applies to the exchange between groups of oscillators (Figure 2). To this purpose, one introduces the notion of subsystem which are groups of oscillators randomly excited by *uncorrelated white noises but with the same level of power spectral density* (rain-on-the-roof excitation).

The usual way to derive the coupling power proportionality in a modal framework is to consider energy equipartition between modes. Let us consider two subsystems containing respectively  $N_1$  and  $N_2$  oscillators (henceforth called modes). In each subsystem, the total vibrational energy  $\langle E_i \rangle$  (with  $i = 1, 2$ ) is the sum of individual modal energies. Furthermore, the power exchanged  $\langle P_{12} \rangle$  is the sum of individual exchanges between any pair of modes (Figure 2). By applying the coupling power proportionality to any pair of modes and by assuming *the equipartition of modal energy* (all modes have the same energy  $\langle E_i \rangle / N_i$ ),

$$\langle P_{12} \rangle = B \left( \frac{\langle E_1 \rangle}{N_1} - \frac{\langle E_2 \rangle}{N_2} \right), \quad (2.4)$$

where factor  $B$  is the sum of individual  $\beta$  for all pairs of modes. Assuming in addition that *the number of modes is large and the damping is light*, the factor  $B$  simplifies. For an elastic coupling, factor  $B$  reads

$$B = \frac{\pi K^2 n_2}{2\omega^2 M_1 M_2}, \quad (2.5)$$

where  $M_i$  the total mass of subsystem  $i$ . The conceptual difference between equations (2.3) and (2.5) is that the former requires the exact values of all natural frequencies of all modes, an information computationally costly in general which is not the case for the latter. This justifies the gain in simplicity and consequently in the computation time in using SEA.

In practice, systems are made of structural components which may be beams, plates, shells, acoustical cavities, etc. And the subsystems are generally chosen as these components. In the modal approach of statistical energy analysis, the vibrational field of each component is projected on the modal basis (blocked modes) so that continuous subsystems are reduced to sets of oscillators. Since the number of modes of continuous structures is infinite, the only further assumption is that the number of modes is truncated. One introduces a frequency bandwidth of analysis in which the power spectral density of excitation is flat. The notion of resonant modes (modes whose natural frequency lies within the frequency band of external excitations) is also introduced. It is assumed that *the only resonant modes contribute to the global response*.

The coupling loss factors are generally difficult to obtain by the modal approach of SEA due to the considerations about distribution of the natural frequencies [13–15]. So, to determine them in all situations of interest, the wave approach of SEA has been introduced. This second approach of SEA is based on geometrical acoustics [16] and is quite similar to Sabine's theory in room acoustics. The frequency is assumed to be sufficiently high to allow an interpretation in terms of rays and the energy exchange at an interface is assessed by solving the reflection and transmission coefficients for plane waves. The coupling loss factors are then determined assuming that *the vibrational fields in all subsystems are diffuse*.

In summary, the wave approach of SEA is mainly based on the diffuse field assumption while the modal approach of SEA is rather based, on rain-on-the-roof excitation and energy equipartition. These assumptions (Figure 3) lead to the same equation of coupling power proportionality (equation (2.4)). This wave/modal duality has been underlined by many authors and has turned out to be a central concept in all subsequent developments in SEA. However, this duality raises many questions as for instance the equivalence of the three aforementioned required assumptions and their respective domain of validity.

The aim of this paper is to examine each hypothesis, to discuss them on some simple examples and evaluate their relevance in regards to the coupling power proportionality.

### 3. SEA Hypothesis

#### (a) Diffuse field

As discussed by Langley [17], two approaches are possible when talking about diffuse field, the wave motion or the resonant modal energy point of view. It leads to different types of definitions. In wave acoustics, Rossi [18] explains that a diffuse field is characterized by a constant sound pressure level during steady state and a linear time decrease spatially independent when sources are switched off. From the geometrical acoustics point of view given by Faller [19], an ideal diffuse sound field is homogeneous and isotropic or, in other words, it is assumed that independent sound waves of equal strength arrive at a receptor (the microphone) from all directions. Lyon [20] proposed a definition of diffuseness from a statistical mechanics point of view where modes are understood as oscillators. When sets of oscillators are taken three conditions must be satisfied : (i) modes are equally energetic within the frequency band, (ii) displacement and momenta of a mode are statistically independent, (iii) the displacements of different modes are statistically independent within the frequency band. Fahy [21] defines diffuse field using the energy density "the average energy density is the same throughout the volume of the enclosure". This will be our

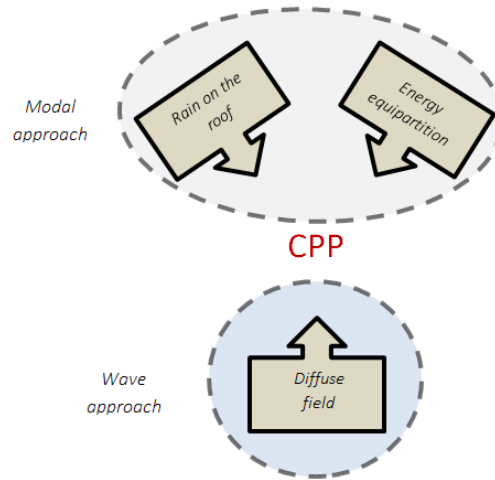


**Figure 3.** Different ways to obtain the coupling power proportionality - a wave-based approach (diffuse field) and a modal-based approach (energy equipartition or rain-on-the-roof).

definition of diffuse field in the present article, the field is considered diffuse if homogeneous. The question of the isotropic nature of a field is not broached here.

### (b) Energy equipartition

In statistical physics, equipartition of energy arises under quite general conditions but provided that non linear interactions between particles ensure the mixing of energy. For instance, in the kinetic theory of gases each particle has a random motion and their energy are shared thanks to their collisions. Remind that equipartition does not mean that all particles (modes in the present context) have the same energy at a fixed time but only that their time-averaged energies are equal [22]. A typical counter-example is precisely the one of linear oscillators since this is a non ergodic system. Magionesi [23], in his discussion on the validity of the energy equipartition for general engineering systems first recall the critical aspect related to the applicability formulated in statistical mechanics. Each system of an ensemble has the same structure and the same physical properties ; the "hypothesis of a uniform probability of finding representative points of the ensemble of systems over equal-energy-surface in the phase space is assumed" and the assumption of weak coupling is considered. He finally summarized the hypothesis where the energy equipartition principle is supposed to hold: for linear homogenous and weakly coupled oscillators, energy equipartition may be possible if the same energy quantity is injected via random forces. Calling  $\langle E_i^A \rangle$  and  $\langle E_k^B \rangle$  the average energies of mode  $i$  in subsystem  $A$  and mode  $k$  in subsystem  $B$ ;  $\langle E^A \rangle$  and  $\langle E^B \rangle$  the global energies;  $N_A$  and  $N_B$  the number of modes, energy equipartition assumption can be written as [24],

$$\langle E_i^A \rangle = \frac{\langle E^A \rangle}{N_A}; \langle E_k^B \rangle = \frac{\langle E^B \rangle}{N_B}. \quad (3.1)$$

### (c) rain-on-the-roof excitation

In the modal approach of SEA the external force distribution is assumed to be statistically independent [1], [12], so that all modes of the structure are excited with the same level. A force field  $f(x, t)$  is called rain-on-the-roof if its autocorrelation function is,

$$R_{ff}(\chi, \tau) = \langle f(x, t)f(x', t + \tau) \rangle = \delta(x - x')\delta(\tau)S_0, \quad (3.2)$$

where  $S_0$  is a constant. Let  $\psi_n$  the mode shape of mode  $n$ , the modal forces  $L_n = \int f\psi_n dx$  has the cross-correlation

$$\langle L_n(t)L_m(t+\tau) \rangle = \iint \psi_n\psi_m \langle f(x,t)f(x',t+\tau)dx dx' \rangle = S_0\delta(\tau)\delta_{nm} \quad (3.3)$$

by virtue of orthonormality of modes so that modal forces are uncorrelated and white noises with same power spectral density  $S_0$ . The converse is also true. Fahy [25] pointed out that the special case of point excitation is not valid for SEA in the sense that it does not lead to the same level of modal forces. A strict rain-on-the-roof field corresponds to an infinite number of uncorrelated excitation points. But numerically, such an external force distribution is reduced to a large number of excitation points placed randomly on the structure. In this paper, a quantification is made to evaluate a "fair" rain-on-the-roof excitation.

#### 4. Case of a simply supported plate

A typical issue in SEA is to compute the vibrational response of a structure excited by a random force field. More precisely, one considers a structure excited by either a point force or a set of random point forces having a power spectral density constant in a frequency band. The main goal is to compute the expectation of the local energy  $\langle e \rangle (x, y, \omega_c)$  which depends on the receiver point  $x, y$  and the frequency band  $\Delta\omega$  centred on  $\omega_c$ . The expectation of modal energy  $\langle E_n \rangle (\omega_c)$  depends on the mode index  $n$  and the centre angular frequency  $\omega_c$ . The diffuse nature of a field can be examined by comparing the energy at different points on the structure while the principle of energy equipartition is fulfilled if all modal energy are equal.

Let us consider a plate having dimensions  $L_x \times L_y$  excited by a set of white noise random transverse point forces. The bending rigidity is noted  $D = Eh^3/12(1-\nu^2)$ ,  $\rho$  the mass density,  $h$  the thickness,  $m = \rho h$  the mass per unit area,  $E$  the Young modulus,  $\nu$  the Poisson ratio. Figure 4 illustrates the test case.

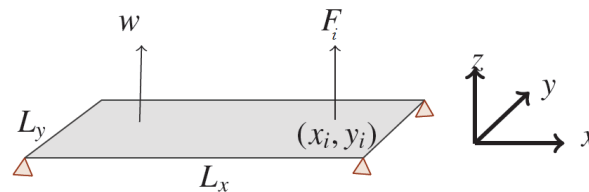


**Figure 4.** Simply supported plate excited by several random forces having the power spectral density of white noise and the output is the deflection at a receiver point.

The equation of motion governing the transverse displacement  $w(x, y, t)$  of an undamped plate excited by a force field  $f(x, y, t)$  is,

$$D\nabla^4 w(x, y, t) + m \frac{\partial^2 w(x, y, t)}{\partial t^2} = f(x, y, t), \quad (4.1)$$

where  $\nabla^4 = \frac{\partial^4}{\partial x^4} + \frac{\partial^4}{\partial y^4} + 2 \frac{\partial^2}{\partial x^2} \frac{\partial^2}{\partial y^2}$ . In the case of  $N$  point sources the force distribution reads

$$f(x, y, t) = \sum_{i=1}^N F_i(t)\delta(x-x_i)\delta(y-y_i), \quad (4.2)$$

where  $F_i$  are random functions whose power spectral density  $S_i(\omega)$  is assumed constant within the frequency band  $\Delta\omega$  and zero elsewhere. Let  $H$  be the frequency response function between  $w$

at  $x, y$  and  $F_i$  at  $x_i, y_i$ . By a modal decomposition and introducing an *ad hoc* damping loss factor  $\eta$  to account for dissipation,  $H$  is given by

$$H(x, y; x_i, y_i; \omega) = \sum_{n \geq 0} \frac{\psi_n(x_i, y_i) \psi_n(x, y)}{m(\omega_n^2 - \omega^2 + j\eta\omega_n\omega)}, \quad (4.3)$$

where  $\psi_n$  denotes the mode shape of mode  $n$ .

### (a) Local energy expectation

The complete expression of the plate energy is given by Soedel [26]. However, for the sake of simplicity one defines the local energy  $e(x, y, t)$  as twice the kinetic energy density. Therefore, the expectation of local energy is

$$\langle e(x, y, t) \rangle = m \langle \dot{w}(x, y, t)^2 \rangle. \quad (4.4)$$

The term  $\langle \dot{w}^2 \rangle$  can be viewed as the autocorrelation function of  $\dot{w}$  taken at zero. This is also the Fourier transform of the power spectral density  $S_{\dot{w}\dot{w}}$  at zero,

$$\langle \dot{w}(x, y, t)^2 \rangle = R_{\dot{w}\dot{w}}(0) = \frac{1}{2\pi} \int_{-\infty}^{+\infty} S_{\dot{w}\dot{w}}(\omega) d\omega. \quad (4.5)$$

But since forces are uncorrelated, the power spectral density of  $\dot{w}$  is related to the power spectral density of forces by,

$$S_{\dot{w}\dot{w}}(\omega) = \sum_{i=1}^N \omega^2 |H|^2(\omega) S_i(\omega), \quad (4.6)$$

Combining equations (4.4), (4.5) and (4.6) gives,

$$\langle e \rangle(x, y, \omega_c) = \sum_{i=1}^N \frac{S_i}{2\pi} m \int_{\Delta\omega} \omega^2 |H|^2 d\omega, \quad (4.7)$$

where the bounds of the integral have been reduced to  $\Delta\omega$  since  $S_i(\omega)$  is zero outside. The mean  $\langle e \rangle$  does not depend on time for stationary forces. One has added  $\omega_c$  as variable to highlight the dependance on centre frequency. The problem comes down to the computation of the frequency response function  $H$  between any two arbitrary points.

### (b) Modal energy expectation

The global energy can be calculated by integrating the local energy over the plate surface. It yields,

$$\langle E \rangle(\omega_c) = \int_0^{L_x} \int_0^{L_y} \langle e \rangle(x, y, \omega_c) dx dy, \quad (4.8)$$

The orthogonality of mode shapes reads  $\int_S \psi_n(x, y) \psi_p(x, y) dx dy = \delta_{n,p}$  where  $\delta_{n,p}$  is Kronecher's symbol. Combining (4.3), (4.7) and (4.8) the expectation of the global energy reduces to

$$\langle E \rangle(\omega_c) = \sum_{n \geq 0} \langle E_n \rangle. \quad (4.9)$$

where the modal energy  $\langle E_n \rangle$  is

$$\langle E_n \rangle(\omega_c) = \sum_{i=1}^N \frac{S_i}{2\pi} \int_{\Delta\omega} \omega^2 \frac{\psi_n(x_i, y_i)^2}{m((\omega_n^2 - \omega^2)^2 + (\eta\omega_n\omega)^2)} d\omega. \quad (4.10)$$



### (c) Diffuse field and energy equipartition criteria

From the distribution of local energy inside a plate, one must estimate whether the field is diffuse or not. To obtain a single criterion, one introduces the standard deviation divided by the mean value of the local energy expectation,

$$\sigma_d = \frac{\sqrt{\langle e \rangle^2 - \langle e \rangle^2}}{\langle e \rangle}, \quad (4.11)$$

where the  $\overline{(\cdot)}$  operator is defined by  $\overline{(\cdot)} = \frac{1}{L_x L_y} \iint (\cdot)(x, y) dx dy$

An analogous approach is adopted with energy equipartition. The criterion is similar to equation (4.11),

$$\sigma_e = \frac{\sqrt{\langle E_n \rangle^2 - \langle E_n \rangle^2}}{\langle E_n \rangle}, \quad (4.12)$$

where now  $\overline{(\cdot)} = \frac{1}{N} \sum_n^N (\cdot)$ . When  $\sigma_d$  or  $\sigma_e$  approaches zero, the local energy is uniformly distributed over the plate or the modal energy is uniformly distributed among modes.

## 5. Numerical results

As first example, let us consider a simply supported rectangular plate having characteristics as shown in Table 1. The excitations have the same power spectral density constant in a octave band centred on  $\omega_c$  and their positions are randomly chosen with a uniform distribution. There are 3000 receiver points which are also randomly chosen. Nine octave bands are considered. For a simply supported rectangular plate, the mode index  $n$  is a double subscript  $(\alpha, \beta)$

type	symbol	value	unit
Dimensions	$L_x \times L_y$	$1.44 \times 1.2$	$m$
Density	$\rho$	7800	$kg/m^3$
Young modulus	$E$	$2.1E11$	$N/m^2$
Poisson ratio	$\nu$	0.3	–
Thickness	$h$	2	$mm$
Damping coefficient	$\eta$	[0.001 – 0.9]	–
Central octave frequency	$f_c$	[16 – 8000]	$Hz$
Frequency step	$df$	$(\eta f_{max})/4$	$Hz$
Mean free path	$l$	1.0282	$m$

**Table 1.** General parameters of the studied plate.

and the expressions of the undamped natural frequencies and the mode shapes are [27]  $\omega_n = \sqrt{D/m} \left( (\alpha\pi/L_x)^2 + (\beta\pi/L_y)^2 \right)$  and  $\psi_n(x, y) = (2/\sqrt{L_x L_y}) \sin(\pi\alpha x/L_x) \sin(\pi\beta y/L_y)$ . The computation of the local energy follows from equation (4.7) with  $S_i = 1$  and  $H$  given by equation (4.3) where  $\psi_n$  and  $\omega_n$  as above. However, in the sum of equation (4.3) only resonant modes (modes within the frequency band) have been considered. All non-resonant modes have been simply neglected. The computation of the modal energy and the equipartition criterion follow respectively equations (4.10) and (4.12) again limited to resonant modes.

### (a) Diffuse field

Recently Le Bot [28] proposed validity diagrams on the frequency-damping space to have an idea of how well the SEA method could be applied to a system. It leans on some specific parameters: the number of resonant modes  $N$  in the frequency band; the modal overlap  $M$  which is defined as the product of the modal density and  $\eta\omega_c$ ; the attenuation factor per unit length

$m = \eta\omega l/c_g$  where  $c_g$  is the group speed of waves and  $l = \pi L_x L_y / 2(L_x + L_y)$  the mean free path; the dimensionless wave number  $\kappa = kl/2\pi$  where  $k = (\omega^2 m/D)^{1/4}$  is the structural wavenumber. Such a representation is used to observe diffuse field.

Figure 5 shows the evolution of diffuse field criterion for a single point force versus  $\kappa$  and  $\eta$ . The dotted line represents the modal overlap  $M = 1$ , the dashed line the attenuation factor  $m = 2$  and the vertical solid line the number of modes  $N = 10$ . The presence of several points (A,B,C,D,E,F and G) is useful for the next paragraphs and sections.

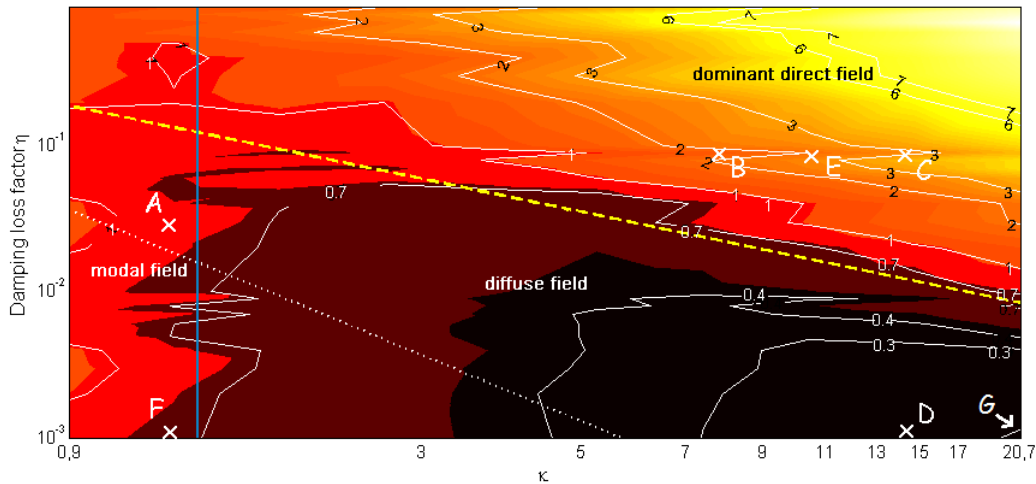


**Figure 5.** Diffuse field criterion for a rectangular plate excited by a single point force versus wavenumber - damping ratio compared to the modal overlap  $M=1$  (dotted line), the attenuation factor  $m=2$  (dashed line) and the number of modes  $N=10$  (vertical solid line).

The  $\sigma_d = 0.7$  contour line defines the area of a quasi-diffuse field. It occurs principally at high frequency and low damping. Above this contour line, increasing the damping, the criterion quickly increases showing a change in the energy field. The field is no more diffuse but is dominated by the direct field emanating from the point force. The 0.7 contour line is almost a straight line above  $\kappa = 1.84$ . As one can see, the dashed line representing the attenuation factor  $m = 2$  fits well with that contour line. At low frequency (below  $\kappa < 1.40$  or  $N < 10$ ) the diffuse field criterion slightly increases. In these first frequency bands, only few modes are resonant and the energy field is dominated by a modal behaviour. The dotted line drawn in Figure 5 shows values for which the modal overlap  $M = 1$  occurs. It is often assumed that for energy methods like SEA, the modal overlap of the structure has to be higher than one. This limit is clearly not correlated to the diffuse field criterion.

Figure 6 shows the evolution of the diffuse field criterion versus the number of point excitations with the same power spectral density. Two cases are tested represented by point A and point B in Figure 5: In Figure 6a the field is modal with a single excitation ( $\kappa = 1.29$ ,  $f_c = 31.5\text{Hz}$ ;  $\eta = 0.03$ ) (point A in Figure 5). In Figure 6b the field is direct ( $\kappa = 7.31$ ,  $f_c = 1000\text{Hz}$ ;  $\eta = 0.1$ ) with a single excitation (point B in Figure 5). In both cases the criterion decreases going below 0.7 drawn in grey when the number of excitations increases (from 1 to 1000). A large number of excitations is a favorable condition for diffuse field. The fact that the criterion tends to non zero limit may be explained by two approximations done in the simulation: first, the limited number of receiver points (3000) and the fact that the kinetic energy is fixed at zero by the boundary conditions. By this second approximation, an outskirts area of the plate have a null energy density. The size of this area depends on wavelength and thus on the frequency band: the lower the frequency, the larger this area.

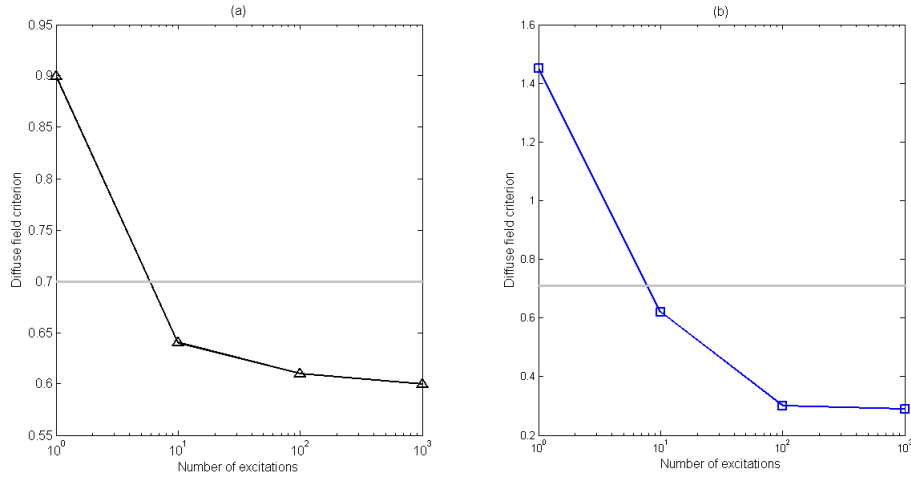


**Figure 6.** Evolution of the diffuse field criterion versus the number of uncorrelated random excitations. (a) From modal field to diffuse field ( $\kappa = 1.29$ ,  $f_c = 31.5\text{Hz}$ ;  $\eta = 0.03$ ); (b) From dominant direct field to diffuse field ( $\kappa = 7.31$ ,  $f_c = 1000\text{Hz}$ ;  $\eta = 0.1$ ).

From Figure 6 it is observed that even if a field is not diffuse for a single excitation ( $\sigma_d > 0.7$ ) it becomes diffuse when a higher number of excitations is used. It means that if a field is not naturally diffuse in a subsystem (modal fields, direct fields) using a rain-on-the-roof excitation would enforce it to be diffuse. Consequently, the hypothesis of a rain-on-the-roof excitation implies the state of diffuse field. The reciprocal is not verified since it has been shown that a field can be naturally diffuse even with a single excitation.

## (b) Energy equipartition

Figures 7 and 8 show the repartition of modal energy in two test cases: point *C*  $\kappa = 14.63$ ;  $\eta = 0.1$  and point *D*  $\kappa = 14.63$ ;  $\eta = 0.001$  from Figure 5. The excitation is either a single (Figure 7) or a group (Figure 8) of random forces.

The repartition of the modal energy when the plate is excited by a single excitation is decreasing and can be fitted with a Weibull distribution. The first order of a such function reads

$$W(x, a, b) = abx^{b-1}e^{-ax^b}, \quad (5.1)$$

where  $a$  and  $b$  are adjustable parameters. 36% to 38% of the total number of modes in the frequency band have a low modal energy value. Very few modes have the maximum of the modal energy ( $\approx 0.3\%$ ). The equipartition criterion  $\sigma_e$  for each case are between 1.1 and 1.2. The frequency range influences the number of modes in the frequency band and the damping coefficient the value of modal energies but the general distribution of modal energy is identical for both cases. In the simulation,  $\eta = 0.1$  (Figure 7a) gives ( $a = 0.006$ ;  $b = 0.063$ ) and  $\eta = 0.001$  (Figure 7b) gives ( $a = 1.201$ ;  $b = 0.049$ ).  $a$  and  $b$  have such values that the Weibull distribution can be approximated by,

$$W(x, a, b) \sim \frac{ab}{x}. \quad (5.2)$$

This clearly shows that equipartition is usually not fulfilled for a single excitation. Figure 8 shows the repartition of modal energy when 10 random excitations are used and for two cases of damping loss factor (point *C* - Figure 8a and point *D* - Figure 8b). These repartition can be fitted

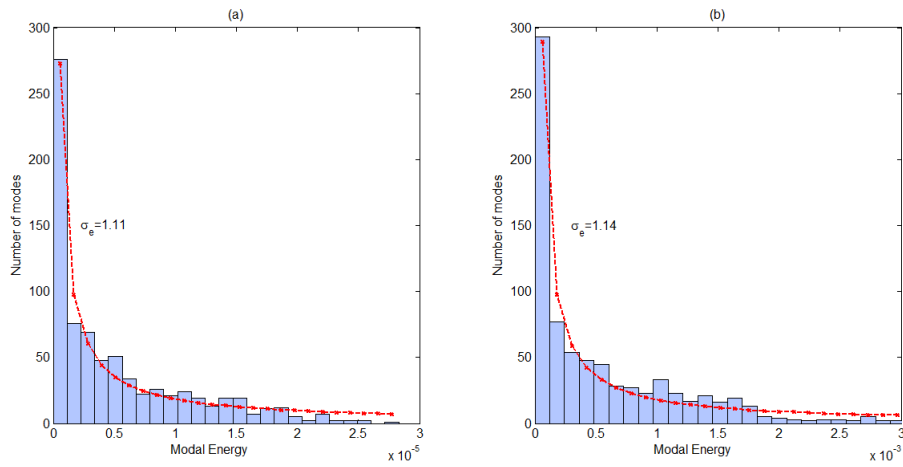


**Figure 7.** Repartition of modal energy for a rectangular plate excited by a single point force. (a) point C: ( $\kappa = 14.63$ ,  $f_c = 4kHz$ ;  $\eta = 0.1$ ) and (b) point D: ( $\kappa = 14.63$ ,  $f_c = 4kHz$ ;  $\eta = 0.001$ ).

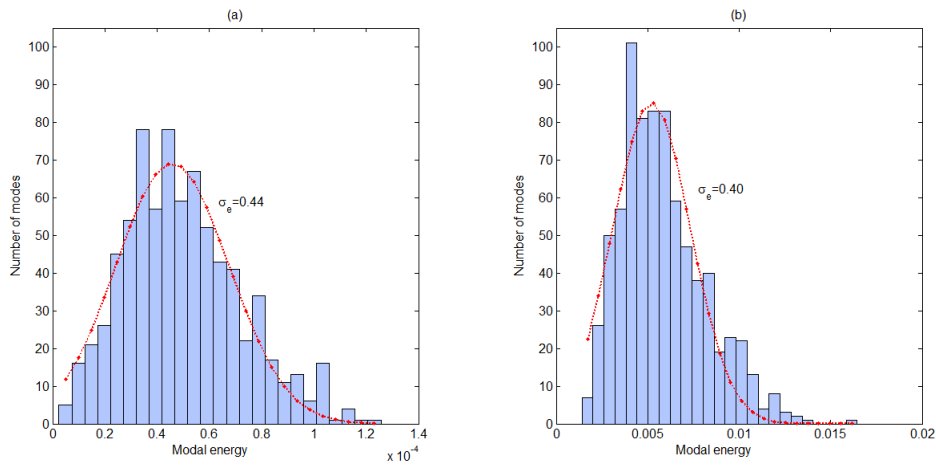


**Figure 8.** Repartition of modal energy repartition for a plate excited by 10 point forces. (a) point C: ( $\kappa = 14.63$ ,  $f_c = 4kHz$ ;  $\eta = 0.1$ ) and (b) point D: ( $\kappa = 14.63$ ,  $f_c = 4kHz$ ;  $\eta = 0.001$ ).

with Gaussian distributions

$$G(x, c, d, f) = ce^{-\left(\frac{x-d}{f}\right)^2}, \quad (5.3)$$

where  $c$ ,  $d$  and  $f$  are adjustable parameters. The case  $\eta = 0.1$  gives ( $c = 69.13$ ;  $d = 4.584E - 5$ ;  $f = 3.071E - 5$ ) and  $\eta = 0.001$  gives ( $c = 85.15$ ;  $d = 5.207E - 3$ ;  $f = 3.025E - 3$ ). The value of damping coefficient does not affect the repartition shape which is now centred on the mean value. The rain-on-the-roof excitation is therefore favorable for equipartition.

The results may be interpreted as follows. The general expression of the modal energy is in the special case of a single excitation,

$$\langle E_n \rangle (\omega_c) = \frac{S_0 \psi_n(x_i, y_i)^2}{2\pi} \int_{-\infty}^{+\infty} \omega^2 \frac{1}{m((\omega_n^2 - \omega^2)^2 + (\eta \omega_n \omega)^2)} d\omega = \frac{S_0 \psi_n(x_i, y_i)^2}{2m\eta \omega_n}. \quad (5.4)$$

where the limit of integration of equation (4.10) have been extended to infinity for simplicity. The modal energy is therefore strongly dependent on the mode by the term  $\psi_n/\omega_n$  which demonstrates that the energy is not equally distributed. On the contrary, for an infinite number of excitations and since  $\lim_{N \rightarrow \infty} (1/N \sum_{i=1}^N \psi_n(x_i, y_i)^2) = 1/(L_x L_y)$ . The expectation of the modal energy is,

$$\langle E_n \rangle (\omega_c) = \sum_{i=1}^N \frac{S_0 \psi_n(x_i, y_i)^2}{2m\eta\omega_n} = \frac{NS_0}{L_x L_y 2m\eta\omega_n} \sim \frac{1}{\omega_n}. \quad (5.5)$$

The modal energy depends on the frequency. Consequently, a constant damping loss factor and a rain-on-the-roof excitation leads to a modal energy which is not equally distributed [29]. But when choosing another damping model, for example the one used by Lyon [1] that is a half-power bandwidth  $\Delta = \eta\omega_n$  constant then the modal energy becomes

$$\langle E_n \rangle (\omega_c) = \frac{NS_0}{L_x L_y \Delta m}. \quad (5.6)$$

In that case the energy is equally distributed between modes, the equipartition of modal energy is reached.

Figure 9 represents the repartition of modal energy for both models of damping. The centre frequency stays at  $f_c = 4000Hz$  and a group of 1000 random excitations is taken. The energy

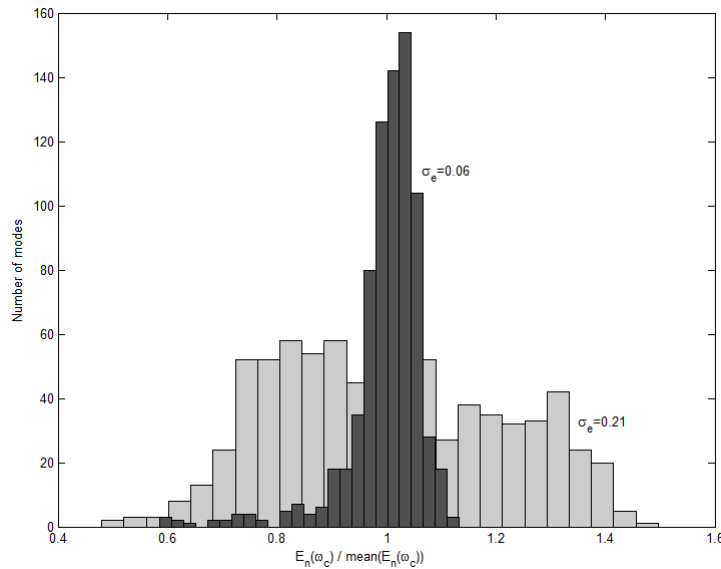


**Figure 9.** Modal energy repartition for a plate excited by 1000 random point forces. The centre frequency is  $f_c = 4000Hz$  and the damping models are different :  $\eta$  is constant ( $\eta = 0.01$ ) - light grey and  $\Delta = 4\pi\eta f_c$  is constant ( $\Delta = 502.65$ )- dark grey repartition.

distribution is drawn in light grey when the modal damping ratio is maintained constant with  $\eta = 0.01$  (diffuse field condition). It corresponds to a Gaussian distribution similar to the one in Figure 8. Otherwise, when the half-power bandwidth defined as  $\Delta = 4\pi\eta f_c = 502.65$  (in dark grey) is maintained constant the modal energy distribution is again a Gaussian but much more tighten showing that the modal energies have closed values. The energy equipartition criterion is in that case three times lower ( $\sigma_e = 0.067$  instead of  $\sigma_e = 0.211$ ). This clearly shows that equipartition is reached when the modal forces have same power spectral density (rain-on-the-roof) and when the half-power bandwidth of modes is the same. The case of coupled subsystem is discussed in [30].

For each damping models two approximations are done: the truncation on the mode number and the number of excitation points which is finite.

This simple simulation on a single plate highlights that energy equipartition is a direct consequence of rain-on-the-roof excitation whereas the diffuse field state can be either reached by suitable values of damping and frequency or forced by a rain-on-the-roof excitation.

## 6. Case of two coupled plates

In this section the expectation of local and modal energies in coupled plates are calculated to quantify the state of diffuse field and energy equipartition but also to evaluate the difference between SEA prediction and the reference calculation on the ratio of global energies. The case of two rectangular simply supported plates coupled by a spring is examined (Figure 10).  $w_A$  and  $w_B$

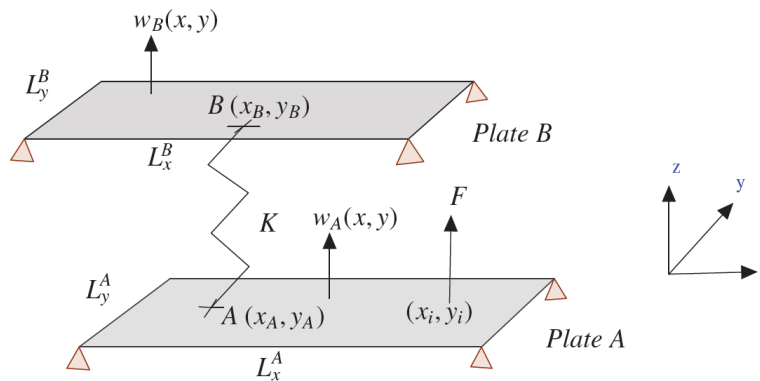


**Figure 10.** Simply supported plates coupled with stiffness  $K$ . Plate  $A$  is excited by a sum of random forces having the power spectral density of white noise.

denote the deflection of plate  $A$  and plate  $B$ ,  $K$  the coupling spring stiffness. If plate  $A$  is excited by a sum of stationary stochastic processes  $f_i(x, y, t)$  which follows equation (4.2), the equations of motion are similar to equation (4.1) with an additional term for the coupling force,

$$D\nabla^4 w_A(x, y, t) + m \frac{\partial^2 w_A(x, y, t)}{\partial t^2} = f(x, y, t) + K(w_B(x_B, y_B, t) - w_A(x_A, y_A, t))\delta(x - x_A, y - y_A), \quad (6.1)$$

for plate  $A$  and

$$D\nabla^4 w_B(x, y, t) + m \frac{\partial^2 w_B(x, y, t)}{\partial t^2} = K(w_A(x_A, y_A, t) - w_B(x_B, y_B, t))\delta(x - x_B, y - y_B), \quad (6.2)$$

for plate  $B$  where  $x_A, y_A$  is the attached point of the spring on plate  $A$  and  $x_B, y_B$  on plate  $B$ .

Let  $G^A(x, y; x_i, y_i, \omega)$  (resp.  $G^B$ ) be the frequency response function of the coupled system for a receiver at  $x, y$  on plate  $A$  (resp. plate  $B$ ) and a unit point force at  $x_i, y_i$  on plate  $A$ . To determine  $G^A$ , one introduces the frequency response functions of uncoupled plates

$$H^A(x, y; x_i, y_i, \omega) = \sum_{n \geq 0} \frac{\psi_n^A(x, y)\psi_n^A(x_i, y_i)}{m(\omega_{A,n}^2 - \omega^2 + j\eta_A\omega_{A,n}\omega)}, \quad (6.3)$$

where  $x_i, y_i$  may be either the position of an external force ( $i = 1, 2, \dots, N$ ) or the position of the coupling spring  $x_A, y_A$  and  $\eta_A, \psi^A$  denote respectively the damping coefficient and the mode shape of isolated plate. The frequency response function for isolated plate  $B$  is similar.

The deflections at any receiver point are given by

$$\begin{aligned} G^A(x, y; x_i, y_i, \omega) &= H^A(x, y; x_i, y_i; \omega) + H^A(x, y; x_A, y_A; \omega)K[W^B(x_i, y_i; \omega) - W^A(x_i, y_i; \omega)], \\ G^B(x, y; x_B, y_B, \omega) &= H^B(x, y; x_B, y_B; \omega)K[W^A(x_i, y_i; \omega) - W^B(x_i, y_i; \omega)], \end{aligned} \quad (6.4)$$

where  $W^A(x_i, y_i; \omega) = G^A(x_A, y_A; x_i, y_i, \omega)$  and  $W^B(x_i, y_i; \omega) = G^B(x_B, y_B; x_i, y_i, \omega)$ . The displacements  $W^A$  and  $W^B$  are found by substituting  $x, y$  with  $x_A, y_A$  and  $x_B, y_B$ ,

$$\begin{aligned} \begin{bmatrix} 1 + KH^A(x_A, y_A; x_A, y_A; \omega) & -KH^A(x_A, y_A; x_A, y_A; \omega) \\ -KH^B(x_B, y_B; x_B, y_B; \omega) & 1 + KH^B(x_B, y_B; x_B, y_B; \omega) \end{bmatrix} \begin{bmatrix} W^A \\ W^B \end{bmatrix} \\ = \begin{bmatrix} H^A(x_A, y_A; x_i, y_i; \omega) \\ 0 \end{bmatrix} \end{aligned} \quad (6.5)$$

Then, the frequency response function  $G^A$  and  $G^B$  at any receiver point are obtained by applying (6.4) with  $W^A$  and  $W^B$  just determined by equation (6.5).

### (a) Local energy expectations

Using equation (4.7) the local energy density  $\langle e \rangle(x, y, \omega_c)$  for plate A is given by

$$\langle e_A \rangle(x, y, \omega_c) = \sum_{i=1}^N \frac{S_i}{2\pi} m \int_{\Delta\omega} \omega^2 |G^A(x, y; x_i, y_i; \omega)|^2 d\omega \quad (6.6)$$

idem for plate B.

### (b) Modal energy expectations

The expectations of the modal energies for the two plates are found using a similar development that was done for a single plate.

$$\langle E^A \rangle(\omega_c) = \int_{L_x^A} \int_{L_y^A} \langle e_A \rangle(x, y, \omega_c) dx dy \quad (6.7)$$

idem for plate B. After calculation the global energy of plate A is

$$\langle E^A \rangle(\omega_c) = \sum_{n \geq 0} \langle E_n^A \rangle(\omega_c) \quad (6.8)$$

where the modal energy expectation is

$$\langle E_n^A \rangle(\omega_c) = \sum_{i=1}^N \frac{S_i}{2\pi} \int_{\Delta\omega} \omega^2 \frac{|\psi_n^A(x_i, y_i) + K\psi_n^A(x_A, y_A)[W^B(x_i, y_i; \omega) - W^A(x_i, y_i; \omega)]|^2}{m((\omega_{A,n}^2 - \omega^2)^2 + (\eta_A \omega_{A,n} \omega)^2)} d\omega, \quad (6.9)$$

for plate A and

$$\langle E_n^B \rangle(\omega_c) = \sum_{i=1}^N \frac{S_i}{2\pi} \int_{\Delta\omega} \omega^2 \frac{|K\psi_n^B(x_B, y_B)[W^A(x_i, y_i; \omega) - W^B(x_i, y_i; \omega)]|^2}{m((\omega_{B,n}^2 - \omega^2)^2 + (\eta_B \omega_{B,n} \omega)^2)} d\omega, \quad (6.10)$$

for plate B.

## 7. Numerical results

The parameters used for the numerical simulation are presented in Table 2. The computation of the expectations of local and modal energies follow the equations (6.6), (6.9) and (6.10). A various number of random excitations is applied on plate A (from 1 to 100) with a uniform distribution. There are 3000 receivers points which are randomly and uniformly placed on both plates. The coupling spring is attached with plate A at  $x_A = 0.72, y_A = 0.6$  and with plate B at  $x_B = 0.38, y_B = 1.06$ . The energy equipartition and diffuse field criteria are computed on each

octave band. Moreover, similarly with the case of a single plate, only resonant modes within the frequency band are taken in the calculation of  $H^A$  and  $H^B$ .

type	symbol	value	unit
Plate A	$L_x^A \times L_y^A$	$1.44 \times 1.2$	$m^2$
Plate B	$L_x^B \times L_y^B$	$1.39 \times 1.1$	$m^2$
Density	$\rho$	7800	$kg/m^3$
Young modulus	$E$	$2.1E11$	$N/m^2$
Poisson ratio	$\nu$	0.3	—
Thickness	$h_A=h_B$	2	$mm$
Coupling stiffness	$K$	981	$N/m$
Mean free path	$l_A$	1.028	$m$
Mean free path	$l_B$	0.964	$m$

**Table 2.** General parameters of the coupled plates

The evolution of the diffuse field and the equipartition criteria for both plates are carried out at high frequency ( $f_c = 2000Hz$ ) and high damping ( $\eta_A = \eta_B = 0.1$ ) (point E from Figure 5) in Figure 11 while the number of random excitation increases. Concerning the diffuse state (Figure

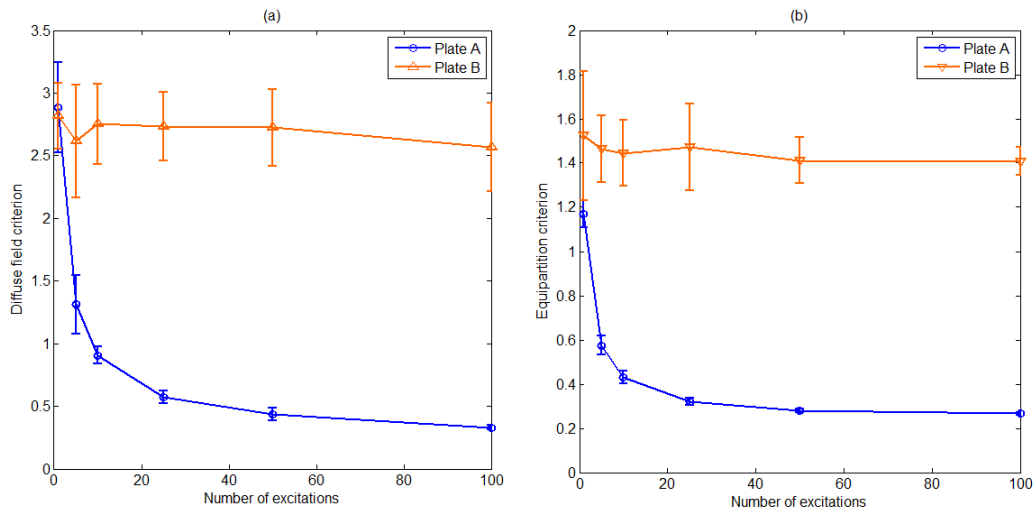


**Figure 11.** Diffuse field and energy equipartition criteria evolution versus number of excitations for two coupled plates at point E: ( $\kappa = 10.35$ ,  $f_c = 2kHz$ ;  $\eta_A = \eta_B = 0.1$ ).

11(a)), results for coupled plates are along the lines of what has been said for a single plate. When plate A is excited by a single point force the diffuse field criterion is high ( $\sigma_d \approx 2.8$ ) indicating a strongly non-diffuse state. The energy is transferred to plate B via the stiffness which acts as a located point force. The diffuse field criterion of plate B has consequently a high value ( $\sigma_d \approx 2.8$ ) and the field in plate B is strongly non-diffuse. When the number of excitations increases up to one hundred the diffuse field criterion of plate A decreases showing that the field becomes diffuse in plate A. But the diffuse field criterion stays high for plate B since the excitation remains a single point force. The dispersion bars are computed for a population of 10 simulations. They are large with few excitations since results are strongly dependent on the excitation and receiver positions.



For the energy equipartition criterion (Figure 11(b)), results are again in agreement with those of an isolated plate: A decrease of the criterion for plate  $A$  is observed meaning that rain-on-the-roof excitation is favorable to equipartition. The dispersion bars are high for both plates with few excitations and quickly decrease. The energy equipartition criterion for plate  $B$  stays high ( $\sigma_e \approx 1.17$ ) since it is still excited by a single source. The modal energy distribution is never equally distributed in plate  $B$ .

## 8. Evaluation of the coupling power proportionality

The global energies ratio given by equation (6.8) are now compared to their SEA predictions.

### (a) SEA approach

For two coupled subsystems  $A$  and  $B$ , where  $A$  is excited by a force field supplying a mean power  $\langle P_A \rangle$ , the energy balance of each subsystem jointly with the coupling power proportionality leads to the standard SEA equation [1],

$$\frac{1}{\omega_c} \begin{pmatrix} \langle P_A \rangle \\ 0 \end{pmatrix} = \begin{bmatrix} \eta_A + \eta_{AB} & -\eta_{BA} \\ -\eta_{AB} & \eta_B + \eta_{BA} \end{bmatrix} \begin{bmatrix} \langle E^A \rangle \\ \langle E^B \rangle \end{bmatrix} \quad (8.1)$$

where  $\eta_A, \eta_B$  are the internal damping of subsystems  $A$  and  $B$ . The coupling loss factors  $\eta_{AB}$  and  $\eta_{BA}$  for two plates coupled by a spring are given by Mace [29]

$$\omega_c n_A \eta_{AB} = \omega_c n_B \eta_{BA} = \frac{K^2}{32\pi\omega^2} \frac{1}{\sqrt{\rho_A h_A D_A} \sqrt{\rho_B h_B D_B}}, \quad (8.2)$$

where  $D_A, D_B$  are the bending stiffness of plate  $A$  and  $B$  and  $n_A, n_B = L_x L_y \sqrt{m/D} / (4\pi)$  are the modal densities. The energy ratio predicted by SEA is therefore,

$$\left( \frac{\langle E^B \rangle}{\langle E^A \rangle} \right)_{SEA} = \frac{\frac{n_B}{n_A}}{1 + \frac{\eta_B}{\eta_{BA}}}. \quad (8.3)$$

### (b) Difference between SEA and reference

The error of SEA compared with the governing equations is,

$$\Delta_{SEA-reference} = \left| 10 \log \left( \frac{\langle E^B \rangle}{\langle E^A \rangle} \right)_{SEA} - 10 \log \left( \frac{\langle E^B \rangle}{\langle E^A \rangle} \right)_{reference} \right|. \quad (8.4)$$

where  $\langle E^B \rangle / \langle E^A \rangle_{SEA}$  is estimated by equation (8.3) and the reference ratio by equation (6.8).

Figure 12 illustrates the error  $\Delta_{SEA-reference}$  for different conditions of simulations (repeated 10 times to compute the dispersion as excitations are randomly distributed). The coupling stiffness varies for each simulation ( $K=981\text{N/m}$  circle marker or  $K=9.81\text{N/m}$  cross marker). The conditions of modal field on plate  $A$  corresponds to point F in Figure 5 ( $f_c = 31.5\text{Hz}$ ,  $\kappa = 1.29$ ;  $\eta_A = \eta_B = 0.001$ ) with a single point force. The error is important whatever the coupling strength is (around  $20\text{dB}$  with a coupling of  $K = 981\text{N/m}$ ) with a large dispersion. The criteria of diffuse field and energy equipartition are  $\sigma_d^A=0.75$ ,  $\sigma_d^B=0.97$ ,  $\sigma_e^A=0.88$  and  $\sigma_e^B=1.23$  showing that these assumptions are not fulfilled. On modal field domain where there is neither diffuse field nor energy equipartition SEA tends to overestimate the energy transfers.

Direct field conditions are set up with large damping coefficient ( $\eta_A=\eta_B=0.1$ ) a high frequency ( $f_c = 4\text{kHz}$ ,  $\kappa = 14.35$ ) and a single excitation (point C in Figure 5). The error is still high ( $\approx 11\text{dB}$ ) as well as dispersion. The criteria show that the conditions of equipartition and diffuse field are not respected ( $\sigma_d^A=3.03$ ,  $\sigma_d^B=3.56$ ,  $\sigma_e^A=1.20$  and  $\sigma_e^B=2.39$ ) which confirms that SEA cannot be used in such a case.

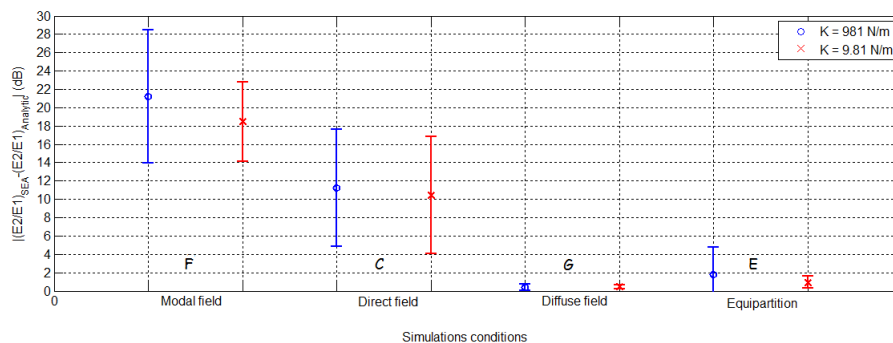


**Figure 12.** Error between SEA and the reference method for several conditions : Modal field - point F: ( $\kappa = 1.29$ ;  $\eta_A = \eta_B = 0.001$ ) 1 excitation ; Direct field - point C: ( $\kappa = 14.35$ ;  $\eta_A = \eta_B = 0.1$ ) 1 excitation ; Diffuse field - point G: ( $\kappa = 29.27$ ,  $f_c = 16 \text{ kHz}$ ;  $\eta_A = \eta_B = 0.0001$ ) 1 excitation ; Energy equipartition - point E: ( $\kappa = 10.35$ ;  $\eta_A = \eta_B = 0.1$ ) 100 excitations

Plate *A* is in diffuse field condition ( $\sigma_d^A = 0.12$  and  $\sigma_d^B = 0.19$ ) when the damping is low, the excitation is single and the frequency band is high (point G). In that case the difference between SEA and reference is near zero which means that a diffuse field state is a sufficient condition for SEA even if neither the hypothesis of rain-on-the-roof nor energy equipartition are fulfilled.

Finally, being in energy equipartition condition (100 excitations,  $\eta_A = \eta_B = 0.1$ ,  $f_c = 2 \text{ kHz}$ ,  $\kappa = 10.35$  represented by point E) permits to apply correctly SEA. The energy equipartition criteria are in that case  $\sigma_e^A = 0.25$  and  $\sigma_e^B = 1.30$ . The measured error range from 1 to 2 dB which may be improved with a lighter coupling stiffness.

## 9. Conclusion

It has been shown that a rain-on-the-roof excitation usually implies a diffuse field state whatever the damping and the frequency band. On the contrary, a point force can produce a diffuse field if the damping is low and the frequency is high. The case of two coupled plates confirms these observations made for a single plate.

The vibrational energy is equally distributed among modes when a rain-on-the-roof excitation is applied provided that the half-power bandwidth is maintained constant. But in the mean time the field becomes diffuse. This observation is valid for all studied frequency/damping cases. Consequently energy equipartition indirectly implies diffuse field.

The two test cases reveal that the assumption with the larger domain of validity is the diffuse field assumption (it consists in the domain of validity of the other assumptions plus the case of a point force under low damping and high frequency). However, one must recall that diffuse field and equipartition are consequences of the type of excitation and the internal properties of the structure (either single excitation in the diffuse field domain or rain-on-the-roof excitation). Assuming diffuse field or energy equipartition allows the use of SEA but is complicated to check a priori. This is why to be sure that SEA may be applied, it is more convenient to assume rain-on-the-roof excitation.

## Acknowledgment

This work was supported by the Labex CeLyA of Universite de Lyon, operated by the French National Research Agency (ANR-10-LABX-0060/ ANR-11-IDEX-0007)

## References

1. Lyon, R. H., Dejong, R. 1995 *Theory and application of Statistical Energy Analysis*. Butterworths-Heimann, Boston, MA.
2. Le Bot, A., Carcaterra, A., Mazuyer, D. 2010 Statistical vibroacoustics and entropy concept. *Entropy* **12**,2418-2435.
3. Le Bot, A. 2009 Entropy in statistical energy analysis *J. Acoust. Soc. Am.* **125**(3),1473-1478.
4. Fahy, F. 1994 Statistical energy analysis: a critical overview. *Phil. Trans. R. Soc. Lond. A* **346**(1681),431-447.
5. Lyon, R.H., Maidanik, G. 1962 Power flow between linearly coupled oscillators *J. Acoust. Soc. Am.* **34**(5),623-639.
6. Crandall, S.H., Lotz, R. 1971 On the coupling loss factor in statistical energy analysis *J. Acoust. Soc. Am.* **49**(1),352-356.
7. Lyon, R.H., Eichler, E. 1964 Random vibration of connected structures *J. Acoust. Soc. Am.* **36**(7),1344-1354.
8. Langley, R.S., Heron, K.H. 1990 Elastic wave transmission through plate/beam junctions *J. Sound Vibrat.* **143**(2),241-253.
9. Wohle, W., Beckmann, TH., Schreckenbach, H. 1981 Coupling loss factors for statistical energy analysis of sound transmission at rectangular structural slab joints, part 1 *J. Sound Vibrat.* **77**(3),323-334.
10. Wohle, W., Beckmann, TH., Schreckenbach, H. 1981 Coupling loss factors for statistical energy analysis of sound transmission at rectangular structural slab joints, part 2 *J. Sound Vibrat.* **77**(3),335-344.
11. Scharton, T. D., Lyon, R. H. 1968 Power flow and energy sharing in random vibration. *J. Acoust. Soc. Am.* **43**(6),1332-1343.
12. Newland, D. E. 1966 Power flow between a class of coupled oscillators. *J. Acoust. Soc. Am.* **43**(3),553-559.
13. Maxit, L., Guyader, J-L. 2001 Estimation of SEA coupling loss factors using a dual formulation and fem modal information, part I: Theory *J. Sound Vibrat.* **239**(5),907-930.
14. Maxit, L., Guyader, J-L. 2001 Estimation of SEA coupling loss factors using a dual formulation and fem modal information, part II: Numerical applications. *J. Sound Vibrat.* **239**(5),931-948.
15. Totaro, N. 2009 SEA coupling loss factors of complex vibro-acoustic systems. *J. Vibrat. Ac.* **131**(4),410091-410098.
16. Le Bot, A. 2007 Derivation of statistical energy analysis from radiative exchanges *J. Sound Vibrat.* **300**,763-779.
17. Langley, R. S., Shorter, P. J. 2002 Diffuse wavefields in cylindrical coordinates. *J. Acoust. Soc. Am.* **112**(4),1465-1470.
18. Rossi, M. 2007 *Audio*. Presses Polytechniques et Universitaires Romandes, Lausanne.
19. Faller, C. 2010 *Signal processing for audio and acoustics*. EPFL, Lausanne.
20. Lyon, R. 1974 A new definition of diffusion. *J. Acoust. Soc. Am.* **56**(4),1300-1302.
21. Fahy, F. J. 1985 *Sound and structural vibration*. Academic, London.
22. Weaver, R.L. 2001 Equipartition and mean-square response in large undamped structure *J. Acoust. Soc. Am.* **110**(2),894-903.
23. Magionesi, F., Carcaterra, A. 2009 Insights into energy equipartition principle in large undamped structures. *J. Sound Vibrat.* **322**(4),851-869.
24. Lesueur, C. 1988 *Rayonnement acoustique des structures*. Eyrolles, Paris.
25. Fahy, F. 1970 Energy flow between oscillators: special case of point excitation. *J. Sound Vibrat.* **11**,481-483.
26. Soedel, W. 2004 *Vibrations of Shells and Plates*. Marcel Dekker, New York.
27. Guyader, J-L. 2002 *Vibrations in continuous media*. ISTE, Paris.
28. Le Bot, A., Cotoni, V. 2010 Validity diagrams of statistical energy analysis. *J. Sound Vibrat.* **329**(6),221-235.
29. Mace, B., Li J. 2007 The statistical energy analysis of coupled sets of oscillators. *Proc. R. Soc. A.* **463**,1359-1377.
30. Ungar, E. 1966 *Fundamentals of statistical energy analysis of vibrating systems*. Technical report, Massachusetts.